

Amyloplast Sedimentation Dynamics in Maize Columella Cells Support a New Model for the Gravity-Sensing Apparatus of Roots¹

Thomas L. Yoder, Hui-qiong Zheng, Paul Todd, and L. Andrew Staehelin*

Department of Astronautical Engineering, United States Air Force Academy, Colorado Springs, Colorado 80840 (T.L.Y.); BioServe Space Technologies Center, Department of Aerospace Engineering Sciences, University of Colorado, Boulder, Colorado 80309-0429 (T.L.Y., P.T.); MCD Biology, University of Colorado, Boulder, Colorado 80309 (H.-q.Z., L.A.S.); and Chemical Engineering, University of Colorado, Boulder, Colorado 80309 (P.T.)

Quantitative analysis of statolith sedimentation behavior was accomplished using videomicroscopy of living columella cells of corn (*Zea mays*) roots, which displayed no systematic cytoplasmic streaming. Following 90° rotation of the root, the statoliths moved downward along the distal wall and then spread out along the bottom with an average velocity of 1.7 $\mu\text{m min}^{-1}$. When statolith trajectories traversed the complete width or length of the cell, they initially moved horizontally toward channel-initiation sites and then moved vertically through the channels to the lower side of the reoriented cell where they again dispersed. These statoliths exhibited a significantly lower average velocity than those sedimenting on distal-to-side trajectories. In addition, although statoliths undergoing distal-to-side sedimentation began at their highest velocity and slowed monotonically as they approached the lower cell membrane, statoliths crossing the cell's central region remained slow initially and accelerated to maximum speed once they reached a channel. The statoliths accelerated sooner, and the channeling effect was less pronounced in roots treated with cytochalasin D. Parallel ultrastructural studies of high-pressure frozen-freeze-substituted columella cells suggest that the low-resistance statolith pathway in the cell periphery corresponds to the sharp interface between the endoplasmic reticulum (ER)-rich cortical and the ER-devoid central region of these cells. The central region is also shown to contain an actin-based cytoskeletal network in which the individual, straight, actin-like filaments are randomly distributed. To explain these findings as well as the results of physical simulation experiments, we have formulated a new, tensegrity-based model of gravity sensing in columella cells. This model envisages the cytoplasm as pervaded by an actin-based cytoskeletal network that is denser in the ER-devoid central region than in the ER-rich cell cortex and is linked to stretch receptors in the plasma membrane. Sedimenting statoliths are postulated to produce a directional signal by locally disrupting the network and thereby altering the balance of forces acting on the receptors in different plasma membrane regions.

For nearly 100 years the dense, starch-filled amyloplasts within the columella cells of the higher plant root cap have been proposed to serve as the gravity-sensing structures of the plant root gravitropic system (Haberlandt, 1900; Nemec, 1900; Darwin, 1903). The sedimentation of these amyloplasts (or statoliths) in response to gravity, and the columella cells (or statocytes) in which they are found, have repeatedly been shown to be necessary for a proper root response to gravity (Pilet, 1971; Sack, 1994; Konings, 1995; Kuznetsov and Hasenstein, 1996; Sack, 1997; Blancaflor et al., 1998; Chen et al., 1999). It is now important to identify mechanisms by which statolith sedimentation might be transduced into a gravitropic growth response.

Theoretical models have been developed for statocyte function (Stockus, 1994; Todd, 1994) but are

hindered by a lack of precise knowledge of the columella cell's biophysical parameters. To act as a sensor, the amyloplast/columella cell combination must be both susceptible to gravity and have a mechanism to respond to it. Because amyloplasts sediment, no doubt exists that they are susceptible to gravity, but questions exist concerning how this is coupled to the response of the columella cell. Of great interest is the means by which the movement of the statoliths in response to gravity is converted to a biochemical signal—the beginning of a transducing chain of events. Therefore, a physical model of the columella cell as a gravitropic sensor must include the mechanism of interaction between the statoliths and other components of the cell, specifically those elements which are known to initiate signal cascades such as the plasma membrane, the endoplasmic-reticulum (ER), and/or the cytoskeletal network.

Numerous models for statolith-statocyte interaction have been proposed over the years. The most popular, referred to as the "tethered" model, postulates that the statoliths are physically connected to cytoskeletal microfilaments that are anchored to the

¹ This research was supported by the National Aeronautics and Space Administration (grant nos. NAG 5-3967 and NCC 8-131), University of Colorado, Boulder.

* Corresponding author; e-mail staeheli@spot.colorado.edu; fax 303-492-7744.

plasma membrane and/or ER (Björkman, 1988; Sievers et al., 1991; Volkmann et al., 1991; Sack, 1994; Todd, 1994; Baluska and Hasenstein, 1997). A modified version of the “tethered” model describes the statoliths not as directly connected, but as sedimenting into a compressed “hammock” of actin fibers (Moore and Evans, 1986; Björkman, 1988). Interaction alternatively may occur through statolith pressures applied to the peripheral ER (Sievers et al., 1991; Sack, 1997).

In this study, we have taken two approaches to evaluate these hypotheses: physical simulation of sedimenting statoliths tethered to actin filaments and light microscopical analysis of the dynamics of sedimenting statoliths and the cytoskeleton in living columella cells. Although this latter approach lacks the resolution to provide direct information about the physical organization of the cytoskeleton in columella cells, it can provide insights into the physical properties of the cytoskeletal matrix via mechanical data. For example, Sack and coworkers (Sack et al., 1985; Sack et al., 1986) observed the kinetics of amyloplast sedimentation in living columella and coleoptile cells of corn (*Zea mays*) by means of videomicroscopy. These studies yielded interesting insights into the behavior of statoliths in response to a 90° reorientation of the growth axis and provided direct information about the average and maximal velocity of sedimenting amyloplasts in such cells. To expand on this work and thereby obtain more detailed insights into statolith-cytoskeletal interactions, we have produced a more precise and more extensive set of video recordings of sedimenting amyloplasts in corn columella cells rotated in all three dimensions. These recordings have been analyzed to provide information on statolith velocity profiles and statolith trajectories in different cellular regions and during different stages of sedimentation. In addition, we have cross-correlated the motion of individual statoliths with each other. It was unexpected that the observational and the simulation studies have yielded results that cannot be readily reconciled with current models. These findings together with new ultrastructural observations have led to the formulation of a hypothesis of statolith-statocyte interactions in which the statoliths are postulated to function not by being connected to the cytoskeleton but instead by being excluded from the cytoskeletal matrix and by their apparent ability to disrupt cytoskeletal interactions within the statocyte.

RESULTS

This “Results” section is divided into three parts. The first describes the movements of the statoliths in living columella cells, the second reports on the ultrastructure of the ER-rich cortical domain and of the cytosolic matrix of the ER-devoid central region of columella cells, and the third presents a mathemati-

cal evaluation of the tethered statolith model of gravity sensing.

Behavior 1: Sedimenting Statoliths Travel Preferentially along the Cell Periphery or through Channels in the Cell Interior

The sedimentation dynamics data presented here were derived from a total of 75 columella cells that included a total of 566 amyloplasts. Roughly half of the experiments involved untreated cells, whereas the other half was treated with cytochalasin D (CD). Figure 1 shows an example of the sedimentation visualization created by the custom software. Figure 1A is an example of a distal-to-side sedimentation profile with the root section initially vertical and subsequently turned horizontally (90°). Figure 1B is an example of a side-to-side sedimentation profile with the section initially horizontal and subsequently turned 180°. In this latter system, the central cytoplasm appears to present an “obstruction” to the sedimentation of the statoliths located in the cell periphery. In response to this obstruction, most statoliths start moving first along the cell periphery toward a site where a lead statolith has made progress in breaching the central obstruction. The congregated statoliths then follow the “leader” across the cytoplasm to the lower side of the cell before dispersing horizontally along the bottom surface of the reoriented cell. This “channeling” was witnessed in every control cell in which the sedimentation profile caused the statoliths to move through the cell’s central region (side-to-side profiles and distal-to-basal profiles following 180° reorientation). Distal-to-side profiles showed no such obstructed behavior.

In qualitative observations, no systematic cytoplasmic streaming was seen in the columella cells, but there was significant diffusive and some minor negative y motion of the statoliths (against gravity). Group-type follow-the-leader behavior of the statoliths occurred in experiments in which they had to transit the cell’s central region in side-to-side and distal-to-basal trajectories. Upon completion of their sedimentation, the statoliths continued to saltate with diffusive motions. Diffusion tended to randomize the arrangements of neighboring amyloplasts, but within a limited distance, with maximum changes in x position being only approximately 20% of the cell’s x dimension during the observation time. Under conditions where statoliths had to move through the cell’s central region, the channeling behavior was observed to various degrees. During the initial stages of statolith movement, which involved significant horizontal motion toward a channel, some statoliths were observed to move upward (against gravity) as if being directed, pulled, or pushed over an obstructing element. This negative y motion was never observed in distal-to-side sedimentation trajectories.

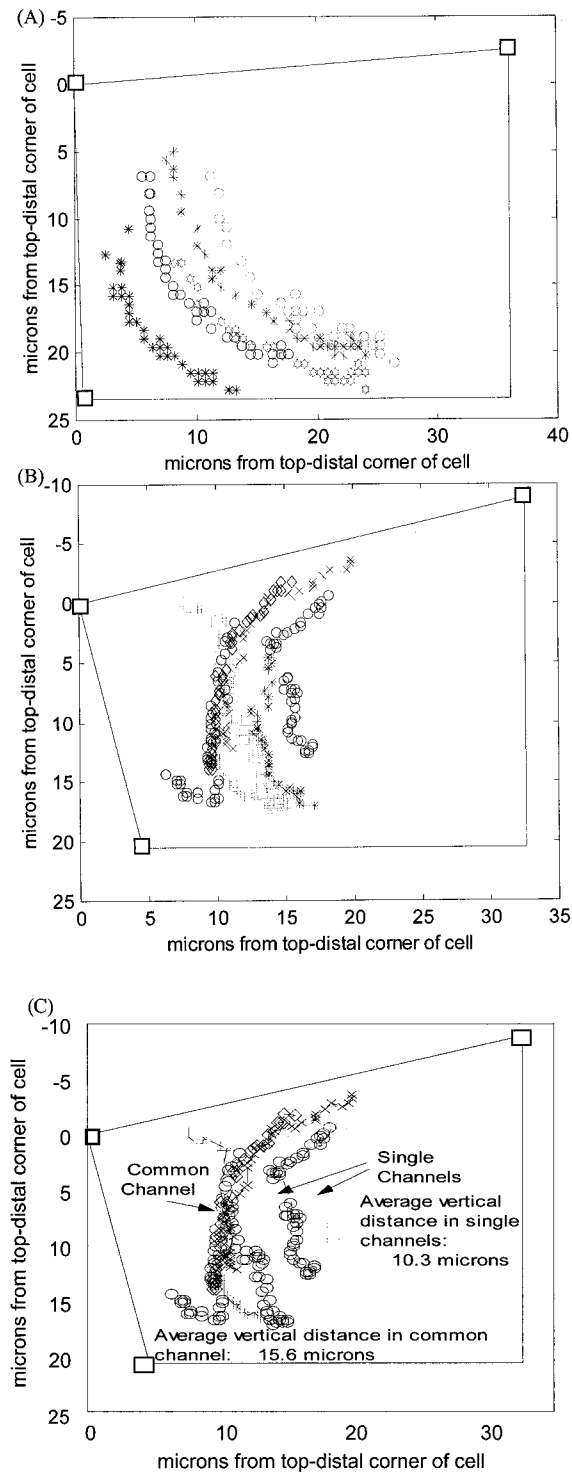


Figure 1. Sedimentation visualized. The shaded boxes define three known corners of the columella cell with appropriate cell walls drawn between. A, Typical distal-to-side movement profile of seven statoliths with 15 s between frames. B, Typical side-to-side movement profile with the nine statoliths falling the entire width of the columella cell with 30 s between frames. C, Identifies those statoliths in B that move either through a common vertical channel or those sedimenting individually through independent channels and shows the average vertical distances covered by statoliths in these two categories.

In three of the columella cells, no statoliths were witnessed to sediment after turning the section 180°. After approximately 15 min, these sections were rotated an additional 10°, placing the distal end slightly down. In all three cases, sedimentation progressed immediately with the statoliths all moving first horizontally toward the cell's distal end and then moving downward along the distal end to the lower side where they came to rest.

Statoliths Travel Faster in Distal-to-Side Than in Side-to-Side Experiments





Statolith velocities were averaged over the first, second, and final third of total sedimentation time. The velocity statistics found within the first and second time windows (approximately 10 min in length) were compared because the statoliths typically completed their sedimentation during the third window. Table I summarizes these data. Of interest is the higher vertical velocity (y velocity) found for statoliths sedimenting along the cell periphery in a distal-to-side trajectory (Student's t test, $P \approx 0.002$). This would indicate less obstruction encountered by the statoliths in the cell periphery. The large standard deviations are attributed to both the significant diffusive saltations observed and imprecision in the data collection method. The x velocities for distal-to-side sedimentation are significantly positive because the statoliths have no option but to move away from the distal cell membrane (positive x velocity). However, in side-to-side sedimentation, average x velocities are near zero because some statoliths move with positive x velocity, whereas others move with negative x velocity as the statoliths approach the channeling sites. No statistical difference ($P > 0.05$) was found between the x or y velocities of statoliths in roots of different lengths. However, even though the component velocities showed less than statistically significant differences, the absolute velocity, the vector magnitude of the two directional components (x and y velocity), appears to differ significantly ($P < 0.04$) between cells from roots with different lengths undergoing similar sedimentation profiles.

Cytochalasin D Alters the Extent of Statolith Channeling

The channeling behavior data are summarized in Table II. The channeling coefficient (CC; "Behavior 1" in "Materials and Methods") provides a measure of the magnitude of overall channeling along the y axis. Only those profiles where the statoliths had to move through the cell's central region (side-to-side and distal-to-basal) were included in these measurements because no centralized channeling behavior was witnessed in distal-to-side sedimentations. On average, the maximum channeling (lowest CC) occurred approximately 12 μm from the top of the cell and

Table I. Statolith velocity statistics (Behavior 1)

Statistics were computed over the first and second thirds of total sedimentation time (time period \approx 10 min). Statistics were compared among the distal-to-side and side-to-side/distal-to-basal sedimentation profiles.

Description	x Velocity	y Velocity	Absolute Velocity
$\mu\text{m min}^{-1}$			
First third of total time			
Distal-to-side profiles ($n = 34$)			
Mean	0.60	1.28	2.38
SD	1.55	1.77	1.75
Side-to-side/distal-to-basal profiles ($n = 240$)			
Mean	0.04	0.58	1.34
SD	1.14	1.21	1.27
Second third of total time			
Distal-to-side profiles ($n = 34$)			
Mean	0.58	0.62	1.65
SD	1.43	1.06	1.36
Side-to-side/distal-to-basal profiles ($n = 240$)			
Mean	0.04	0.56	1.15
SD	0.87	1.09	1.08

approximately 9 μm from the cell's distal end. In untreated roots, the average CC was approximately 0.5 meaning that, on the average, the statoliths were channeled to one-half their original horizontal distribution. Even though this channeling is significant, the calculation takes into account all statoliths tracked within a given cell, including those that are not directed into a common channel. Therefore, this magnitude for channeling is somewhat conservative. For example, the CC for the cell displayed in Figure 1B is shown in Figure 2A and is equal to approximately 0.6 at 5 μm down from the top. Note that the statoliths on the right do not enter the main channel observed on the left, and therefore the histogram of CC is significantly affected by those outlying plastids. However, if only those plastids on the left are included, the magnitude of channeling becomes much more pronounced (Fig. 2B), showing a compression of statoliths into a channel that is one-tenth the width of their original distribution. The individual statoliths that do not participate in channeling are also seen to sediment considerably more slowly than those that move through the main channel (Fig. 1C). Roots treated with CD displayed significantly less channeling ($P = 0.01$), with a mean CC indicating about one-half as much channeling in untreated roots.

Behavior 2: Statolith Movements Are Correlated

Table III summarizes the measurements of correlation coefficients designed to quantify group behavior between the statoliths (Behavior 2 in "Materials and Methods"; correlations of y position over time and y velocity over time). The custom software found the minimum, maximum, mean, and SD of the correlation coefficients between all statolith pairs in a single cell, and the statistics shown in Table III reflect the compiling of these data for all columella cells in a particular group. Note that the correlation between statolith y velocities was significantly lower (0.24–0.50)

Table II. Statolith channeling statistics within columella cells (Behavior 1)

Description	Channeling Coefficient	
	Maximum channel	Location (y)
		μm
Untreated roots ($n = 31$)		
Mean	0.71	11.45
SD	0.28	6.64
With CD ($n = 25$)		
Mean	1.00	12.76
SD	0.40	6.17

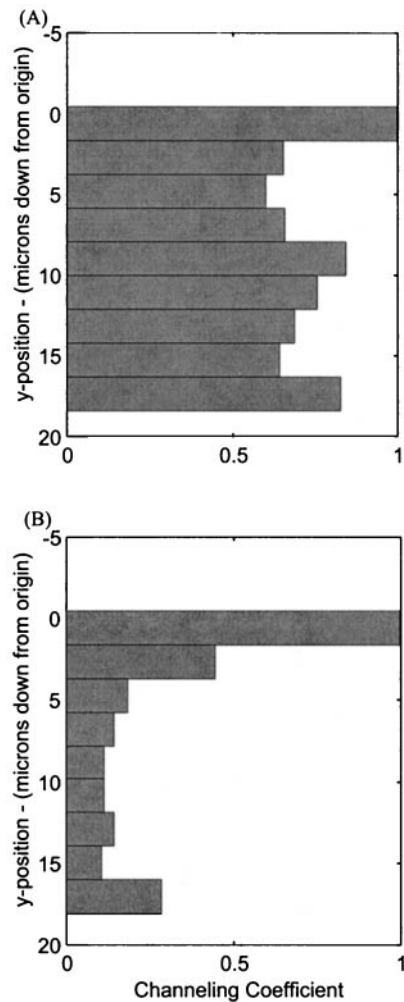


Figure 2. CCs. A, Histogram of CCs for the cell shown earlier in Figure 1B. B, The more significant channeling magnitude that computes when only specific amyloplasts, following the common channel at $x = 10 \mu\text{m}$ in Figure 1B, are included. Low CC (Eq. 3) signifies a common channel.

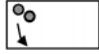

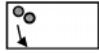

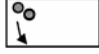

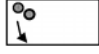

than the correlation between statolith y positions (0.88–0.91). This was expected because y velocity over time ($\Delta v/\Delta t$) is subject to more noise from both data acquisition technique and diffusion. With this in mind, the existence of velocity correlations found in some cells on the order of 0.5–0.7 was much higher than expected. It was evident that some plastids (at a minimum) were acting as a group. The statolith y position correlations confirmed this. If the plastids fall unobstructed, similarly to marbles in a can, this correlation would be close to 1.0. However, if plastids are falling through a random network of cytoskeletal components, this value should be much lower unless the plastids are under the influence of grouping forces, localized open domains in the network, or the bulk flow of cell fluid displaced by the sedimenting statoliths. Table III shows that y position was highly correlated between pairs of statoliths. It is significant that trajectories of

amyloplasts sedimenting in the distal-to-side profiles were more highly correlated than those sedimenting in trajectories across the cell center ($P = 0.015$). In addition, the y velocity correlation of those statoliths traversing the cell centers of untreated roots is significantly lower ($P = 0.0024$) than in those treated with CD. These two statistically significant differences appear to confirm the existence of actin-containing cytoplasmic structures in the central region of columella cells that affect statolith sedimentation.

Behavior 3: Statoliths Move at Different Velocities in Different Locations

Behavior 3, velocity of the amyloplast within various vertical domains of the cell, is summarized in Table IV. The table is divided into two categories, untreated roots and those treated with CD, and two subcategories, distal-to-side and side-to-side (or distal-to-basal) trajectories. Those statoliths undergoing sedimentation in a distal-to-side trajectory exhibited foreseen dynamics, with the statoliths moving the fastest upon gravistimulation and slowing monotonically ($P = .03$ between the top and center sectors; sectors 1 and 3) as they fell closer to the lower side of the cell (Fig. 3A). However, those statoliths moving across the cell's central region (side-to-side or distal-to-basal) start sedimenting at significantly lower speeds ($P < 0.001$), fall most rapidly near the cell center, and slow upon approaching the lower side of the cell (Fig. 3B). During these latter sedimentations, the velocity within the third (or center) vertical sector is significantly higher ($P < 0.001$) than in the first (top) sector. This higher velocity in the cell center correlates with the mean channel location ($y \approx 11\text{--}12 \mu\text{m}$ from the top wall) presented in Table II. The principal effect of CD on the side-to-side sedimentation process appeared to be a hastening of channel formation, as evidenced by the statoliths reaching maximum velocity already in the second sector versus the third sector in control cells (Table IV). The difference between velocities in the second sector in untreated versus CD-treated roots was significantly different ($P = 0.005$). However, the maximum velocity in the third sector remained unchanged in the CD-treated roots. In distal-to-side sedimentation experiments, where the statoliths remained near the cell periphery, the profiles of CD-treated roots show a significant decrease in sedimentation rates ($P < 0.001$) in the top four sectors. This reduction probably reflects the reported effects of CD on the spatial organization and distribution of ER, Golgi, and mitochondria in columella cells (Zheng and Staehelin, 2001) and the resulting interference of these organelles with the sedimentation process (see also next section).

Table III. *Stalolith* group behavior statistics as indicated by velocity and position correlation coefficients (Behavior 2)

Description	Correlation Coefficients	
	Mean	SD
y Velocity correlated over time, untreated roots Distal-to-side profiles ($n = 6$)		
Mean	0.50	0.15
SD	0.11	0.07
Side-to-side and distal-to-basal profiles ($n = 31$)		
Mean	0.24	0.13
SD	0.07	0.03
y Velocity correlated over time, treated with CD Distal-to-side profiles ($n = 13$)		
Mean	0.39	0.16
SD	0.15	0.03
Side-to-side and distal-to-basal profiles ($n = 35$)		
Mean	0.32	0.15
SD	0.10	0.04
y Position correlated over time, without CD Distal-to-side profiles ($n = 6$)		
Mean	0.91	0.08
SD	0.08	0.07
Side-to-side and distal-to-basal profiles ($n = 31$)		
Mean	0.88	0.10
SD	0.10	0.09
y Position correlated over time, with CD Distal-to-side profiles ($n = 13$)		
Mean	0.92	0.07
SD	0.07	0.08
Side-to-side and distal-to-basal profiles ($n = 25$)		
Mean	0.91	0.08
SD	0.06	0.07

The ER of Columella Cells Is Confined to the Cell Cortex in the Form of a Dense, Organelle-Excluding Tubular Network

The root cap of 2.5-d-old corn seedlings (root length 35–45 mm) possesses up to nine tiers of columella cells. The columella cell shown in Figure 4 is from a fifth tier cell layer. In this cell, the ER is confined to a precisely demarcated cortical region of the cytoplasm (Fig. 4, A and B). Most of the ER cisternae exhibit a tubular conformation and are connected to interspersed sheet-like domains, which display a higher density of bound polysomes. The two arrows seen in Figure 4C highlight the remarkably sharp transition between the ER-rich cortical region and the ER-devoid central region of the cell. The ER-rich cortical zone excludes selected types of or-

ganelles, most notably amyloplasts, Golgi stacks, and vacuoles, from approaching the plasma membrane. In contrast, mitochondria, lipid bodies, and small vesicles are evident both in the central and the cortical regions. The confinement of the amyloplasts to the cytosol-rich central region suggests that the low-resistance pathway for amyloplast movement in the cell periphery is associated with the interface between the central region and the ER-rich cortical zone. The cytosol in the central region is characterized by the absence of microtubules and actin filament bundles; instead it appears to be composed of a meshwork of fine microfilaments within which single, straight, and randomly distributed actin-like filaments can be discerned in cryofixed/freeze-substituted cells (Fig. 4D). Taken together, our micro-

Table IV. Summary of statolith velocities within five vertical cellular sectors (Behavior 3)

Description	Top Sector	Sector No. 2	Sector No. 3	Sector No. 4	Bottom Sector
$\mu\text{m min}^{-1}$					
Untreated roots ($n = 274$)					
Distal-side ($n = 34$)					
Mean	1.73	1.71	1.34	1.18	0.68
SD	0.70	0.96	0.76	0.63	0.32
Side-to-side ($n = 240$)					
Mean	0.77	0.82	0.96	0.86	0.68
SD	0.36	0.37	0.45	0.37	0.23
Treated with CD ($n = 292$)					
Distal-side ($n = 77$)					
Mean	0.70	0.87	0.62	0.53	0.36
SD	0.23	0.43	0.16	0.10	0.10
Side-to-side ($n = 215$)					
Mean	0.69	0.91	0.94	0.70	0.47
SD	0.19	0.26	0.33	0.16	0.14

graphs demonstrate that the ER-rich cortical cytoplasm and the ER-devoid central region of columella cells differ greatly in organelle composition and organelle-to-cytosol ratio. This finding provides a morphological basis for explaining the different types of amyloplast trajectories described in the preceding sections.

Physical Simulation of the Tethered Statolith Model of Gravity Sensing Highlights Its Limitations

While physical models can provide valuable insights into the actual physics at work within the gravisensing cells, they are currently limited by a lack of precise knowledge of the columella cell's biophysical properties. One of these properties is the nature of the interaction between the statoliths and the columella cell, or how statolith motion is transmitted to the signal apparatus of the cell through the cytoskeletal apparatus. Without some kind of interaction it is difficult to conceive how the statoliths, although susceptible to gravity, could act as the gravity sensors because their motion could not be imparted to the signaling apparatus of the cell. If a model of the statolith within the statocyte is derived from a balance of forces acting upon the statolith (see Fig. 5), Equation 1 shows the forces at work on the statolith under 1g:

$$\begin{aligned} \Sigma F_y &= ma_y \\ F_g - F_d - F_b - F_e &= ma_y \end{aligned} \quad (1)$$

where $F_g = m_{\text{amy}} g \equiv V_{\text{amy}} \rho_{\text{amy}} g \equiv$ amyloplast weight, $F_d = 6\pi r_{\text{amy}} \eta v \equiv$ Stokes' drag force, $F_b = V_{\text{amy}} \rho_{\text{cyto}} g \equiv$ buoyant force, $F_e \equiv F_{\text{actin}}$ (for interaction with only elastic actin cytoskeletal fibers), m_{amy} = amyloplast mass (kg), V_{amy} = amyloplast volume (μm^3), ρ_{amy} = amyloplast density ($\text{kg}/\mu\text{m}^3$), r_{amy} = amyloplast radius (μm), g = acceleration due to gravity ($9.81/\text{s}^2$ at sea level), η = cytoplasmic

viscosity (centi-poise or Pa s), ρ_{cyto} = cytoplasmic density ($\text{kg}/\mu\text{m}^3$), and v = velocity of the sedimenting amyloplast ($\mu\text{m s}^{-1}$).

Equation 2 shows the complete second-order equation of motion describing the dynamics of amyloplast movement under separate viscous and elastic forces:

$$\ddot{y} + \frac{6\pi r_{\text{amy}} \eta}{m_{\text{amy}}} \dot{y} + \frac{F_{\text{actin}}}{m_{\text{amy}}} = \frac{V_{\text{amy}} g_y \Delta \rho}{m_{\text{amy}}} \quad (2)$$

Most of the biophysical parameters required to accurately model the statolith dynamics have been determined to varying degrees of accuracy, such as amyloplast density (Leach and Schoch, 1961; Robinson, 1985; Wayne et al., 1990) and maize and white-clover statolith dimensions (Moore, 1986; Smith, 1996; Smith et al., 1997). If cytoplasmic viscosity is assumed to be 5 to 20 cP (Sack et al., 1985), the elastic forces due to interaction with the cytoskeletal network (F_{actin}) remain to be characterized.

Assuming the interaction scheme follows the directly "tethered" model, where the statoliths are physically connected via actin filaments to the plasma membrane, a computer simulation was constructed to compare the simulated statolith dynamics to those directly observed under 1g (approximately 10- μm movement with average velocities of 1.5 $\mu\text{m min}^{-1}$). The computer model initially assumed only a single actin fiber connected to each amyloplast and the flexural rigidity of the fiber to be 7.29×10^{-26} nm^2 (Gittes et al., 1993). By assuming homogeneity and an elliptical cross-sectional area (A_{cs}) for the actin fiber of 1.88×10^{-5} μm^2 (Janmey et al., 1991; Gittes et al., 1993; Alberts et al., 1994), this equated to an elastic modulus (E_{actin}) of approximately 2.8 GPa (similar to polyvinylchloride, for example). The elastic force imparted on the plastid by the actin fiber was therefore $E_{\text{actin}} A_{\text{cs}} \epsilon$, where ϵ is the strain imparted on the actin fiber as it is deformed by the statolith. To duplicate the gross dynamics witnessed

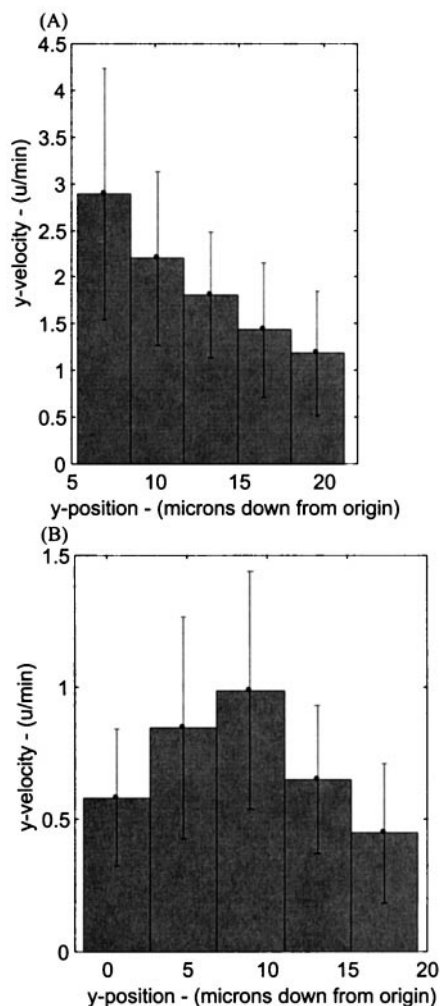


Figure 3. Velocity of statoliths within five vertical sectors of the cell. A, Typical results of a cell undergoing a distal-to-side sedimentation profile. B, Typical results for a cell oriented to produce side-to-side sedimentation of statoliths.

in sedimenting amyloplasts, the model required that the elastic modulus be decreased 10^6 -fold. The dynamics observed in cress during the TEXUS rocket experiments (Volkman et al., 1991) were also used for comparison against simulation results. To attain those gross dynamics (statoliths moving approximately $3.5 \mu\text{m}$ during a microgravity period of 6 min with a maximum speed of $1.4 \mu\text{m min}^{-1}$ and average speed of $0.7 \mu\text{m min}^{-1}$), the elastic modulus again had to be decreased 10^6 -fold. This indicates one of two possibilities: Either the established elastic properties of actin are grossly in error (consider actin filament polymerization and acto-myosin cross-link half-lives) or the "tethered" statolith model is inappropriate. Because we doubt that our calculations are off (for a simple, no cross-linked tether model) by a factor of 10^6 , we assume in the following discussion that the "tethered" statolith model (assuming a permanent, direct statolith-actin-plasma membrane connection) is inaccurate.

DISCUSSION

The principle goals of this study were to obtain quantitative information on statolith sedimentation kinetics in living columella cells and to evaluate these findings in the context of other information on the gravity-sensing apparatus of such cells. Our findings include novel information pertaining to the physical properties of the cytoskeletal system of such cells—quantitative information about statolith kinetics and trajectories, the effects of the actin filament-disrupting drug, CD, on statolith sedimentation, and differences in cytoplasmic organization between the cortical and central regions of the cells. The new experimental insights have led to the formulation of a new hypothesis of gravity sensing by columella cells.

Columella Cells Contain a Low-Resistance Pathway for Statolith Movement in the Cell Periphery

All qualitative and quantitative observations made in this study appear to support a statolith-cytoskeletal interaction scheme that involves a higher degree of statolith obstruction in the central region than in the periphery (especially the distal end) of columella cells. Support for this hypothesis has come from three types of observations: statolith channeling behavior, tracings of statolith trajectories, and statolith velocity measurements (Tables I, II, and IV). In cells that were initially vertical and subsequently turned horizontal (distal-to-side sedimentation), statoliths moving in the cell periphery along the distal end onto the cell's lower side displayed significantly higher velocities than those statoliths traversing the cell center during side-to-side or distal-to-basal sedimentations (Table I). Also, as depicted in Figure 1B, the channeling behavior evidenced in side-to-side experiments involves initially a significant amount of horizontal motion of the statoliths toward the forming channel where they assume a vertical motion toward the cell's lower side. Channeling occurred in only side-to-side (or distal-to-basal) profiles and began at least $5 \mu\text{m}$ from the cell membrane. On average, this channeling reduced the horizontal distribution of statoliths to one-half of its initial width. In a few side-to-side sedimentation experiments, no sedimentation was observed even after 15 min of reorientation. However, when the tips of such roots were tilted slightly downwards, the statoliths in these "non-responding" columella cells started traveling downwards along what appeared to be a least-resistance pathway adjacent to the upper cell wall, then along the near-vertical distal wall, and finally along the bottom of the cell where they came to rest. Taken together, all of these sedimentation responses are consistent with the notion of the peripheral cytoplasm being less obstructive to statolith movement than the cell interior.

Although the exact nature of the low-resistance pathway in the cell periphery is not known, we may

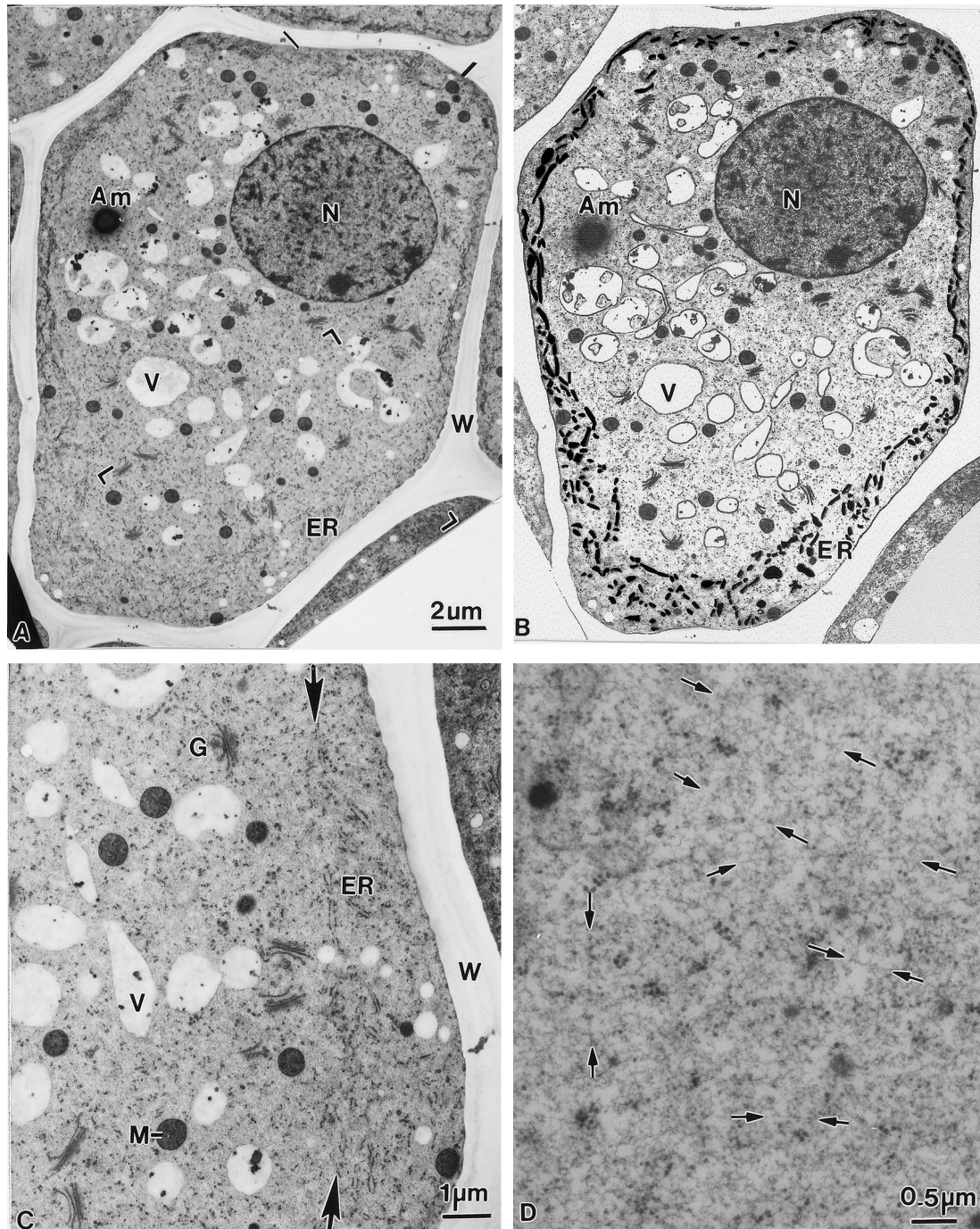


Figure 4. Electron micrograph of a columella cell (A) in a longitudinal section through a corn root tip, and the same micrograph (B) in which the major organelles have been traced to highlight their distribution and particularly the distribution of ER membranes in the cell cortex. Note the distinct differences in organelle distribution between the ER-rich (black lines) cortical zone and the ER-devoid central region. The bracketed area of A is shown at higher magnification in C. The ER cisternae in the cortical region are mostly of the tubular type and carry limited numbers of polysomes, whereas the cytoplasm in the central region exhibits randomly distributed Golgi stacks, mitochondria, and vacuolar profiles. The sharp interface between the cortical and the central regions of the cell is marked with arrows (D). Higher magnification view of the cytosolic matrix material that fills most of the ER-devoid central region of a columella cell and extends between the cortical ER tubules to the plasma membrane. The matrix appears to be comprised of molecules organized in the form of a fine meshwork of straight, randomly oriented filamentous structures (arrows) that resemble actin filaments. N, Nucleus; Am, amyloplast; V, vacuoles; W, cell wall; G, Golgi; M, mitochondria; ER, endoplasmic reticulum.

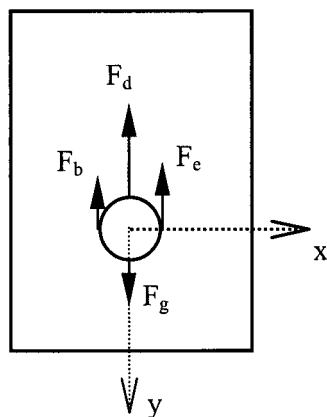


Figure 5. Balance of forces acting on a statolith. F_g is the force due to gravity, F_b is the buoyant force, F_d is the force due to drag, and F_e is the elastic force from cytoskeletal (or other organelle) interaction (a total force possibly composed of both tensile and compressive forces).

speculate on its origin based on the cellular structures known to be present in the cortical cytoplasm (Figs. 4, B and C) and the evidence presented in the next section for the “obstructive material” in the cell center being an actin-based cytoskeletal network (Fig. 4D). Because the cytoplasm underlying the plasma membrane is highly enriched in interconnected tubular ER membranes that form a sharp interface with the cytosol-rich and ER-devoid central region (Fig. 4B), the reduced obstruction of statolith movement in the cell periphery is most likely related to a change in the physical organization of the fine-filamentous cytoskeletal network at the interface between the cortical and central cellular domains.

An Actin-Based Cytoskeletal Network Obstructs Statolith Sedimentation in the Central Region of Columella Cells

To further characterize the nature and properties of the obstructive material in the cell center, we have quantitatively analyzed and mathematically modeled the channeling response as well as investigated how this response is affected by the actin filament disrupting drug CD (Figs. 2 and 3; Tables II and IV). In addition, we have investigated the nature of the cytoskeletal matrix within the central region of cells preserved by high pressure freezing/freeze-substitution methods (Fig. 4D).

The average location of maximum channeling was found to be at approximately the vertical middle of the cell (Table II). This suggests that the density of the movement-obstructing material is greatest near the cell center. However, because channeling was observed to occur along the entire horizontal length of the cells, including the basal end, the movement-obstructing zone must extend throughout the entire

central region. In addition, because the statoliths of untreated roots displayed a significantly higher degree of channeling behavior than those treated with CD, we postulate that an actin-based network is most likely responsible for the channeling effect.

While quantifying the vertical velocity of statoliths in different vertical sectors (Table IV), we found that the distal-to-side sedimentation experiments produced no surprises. These statoliths exhibited the highest velocity ($\approx 1.7 \mu\text{m min}^{-1}$) in the starting (top) sector and monotonically slowed down as they fell into the lower ones and were deflected in a horizontal direction. However, during side-to-side and distal-to-basal sedimentation, the statoliths achieved their lowest velocities in the top sector (presumably because of being obstructed by the underlying cytoskeletal network in the cell’s central region), but sped up once a channel was established and they approached the cell’s center, slowing again upon reaching the bottom of the cell. In roots treated with CD, the vertical velocity of statoliths increased significantly earlier, occurring in the cell’s upper one-third rather than in the cell’s center (Table IV). This result also points to a role of actin in producing the central obstruction and supports earlier reports of increased sedimentability of plastid-based statoliths in cress roots treated with cytochalasins (Sievers et al., 1989).

Both statolith velocity and increase in velocity were found correlated among statoliths (Table III), with velocity correlation being extremely high (>0.9), despite the established obstructive environment. Given no inter-plastid collisions or interaction with any other organelle, velocity correlation should be nearly 1.0 for 1g sedimentation, with diffusion accounting for some deviation from perfect association. Under highly obstructed motion, the case we have established within the columella cell, velocity correlation should be low, with individual statoliths moving independently through the obstructed environment. However, our observations of high velocity correlation between these statoliths (Table III) support either a direct (tethering) or indirect (effects of surrounding cytoskeletal network) grouping influence acting upon the plastids.

Although these findings do not directly address the question of actin organization in columella cells, they do support a scheme in which the actin-based cytoskeletal network is fairly evenly distributed throughout the central cytosol. Further support for this idea has come from the appearance of the cytoskeletal matrix in cryofixed/freeze-substituted columella cells and from both light- and electron-microscopic immunolabeling experiments with antiactin antibodies. As illustrated in Figure 4D, the cytoskeletal matrix of cryofixed cells exhibits a meshwork-like architecture that incorporates randomly oriented, single, straight actin-like filaments but not actin cables. An absence of major actin cables

has also been noted in immunofluorescence labeling studies, which report mostly a diffuse staining of the columella cell cytoplasm (Baluska et al., 1996). Driss-Ecole et al. (2000) most recently have shown that after immuno-gold labeling of chemically fixed and permeabilized columella cells, the gold particles appear organized into short, randomly oriented rows consistent with distribution of the actin-like filaments depicted in Figure 4D. Finally, the lack of systematic cytoplasmic streaming in columella cells (Sack et al., 1986; this study) further substantiates the hypothesis of a network-type organization of the single actin filaments in the central region of columella cells.

Do Statoliths Enlarge the Cytoskeletal Network Pores to Form Channels by Localized Pressure or by Enzyme Action?

Careful examination of the statolith trajectories of the side-to-side sedimentation experiment depicted in Figure 1B highlights yet another aspect of statolith channeling, namely that statolith grouping can accelerate channel formation and sedimentation velocity. This effect can be most readily seen by comparing the length of the trajectories of the statoliths that pass through a channel as a group with the length of the trajectories of individual statoliths that pass through their own channels (Fig. 1C). Channels produced by individual statoliths during a given time period appear much shorter than those involving the participation of multiple statoliths. On the average, statoliths sedimenting through a channel as a group travel over twice as far as those that traverse the cell in regions isolated from the main body of statoliths. This result suggests that the gravitational force available to individual statoliths for breaking through the network lattice is only slightly greater than the forces holding the network together, and that groups of statoliths that congregate at the same channel initiation site can act in concert to enhance the localized pressure and thereby accelerate the channel-forming process and ultimately sedimentation.

In mechanistic terms, the creation of channels through the central actin-based network by statoliths exerting a localized pressure is most likely coupled to the dynamic properties of the network-forming molecules. This is suggested by the fact that most actin filaments have half-lives of approximately 1 min (Theriot and Mitchinson, 1991) and most cross-links between filaments last less than 1 s (Wacksstock et al., 1994). This would enable the statoliths to sediment through the network by passively exploiting the natural turnover dynamics of the actin network, that is, by holding open the otherwise transiently enlarged pores. An actin-based network model of the central region cytoskeleton of columella cells can also explain the faster initial rate of penetration of statoliths into the central region of CD-treated cells, since such a treatment should increase the pore size of the

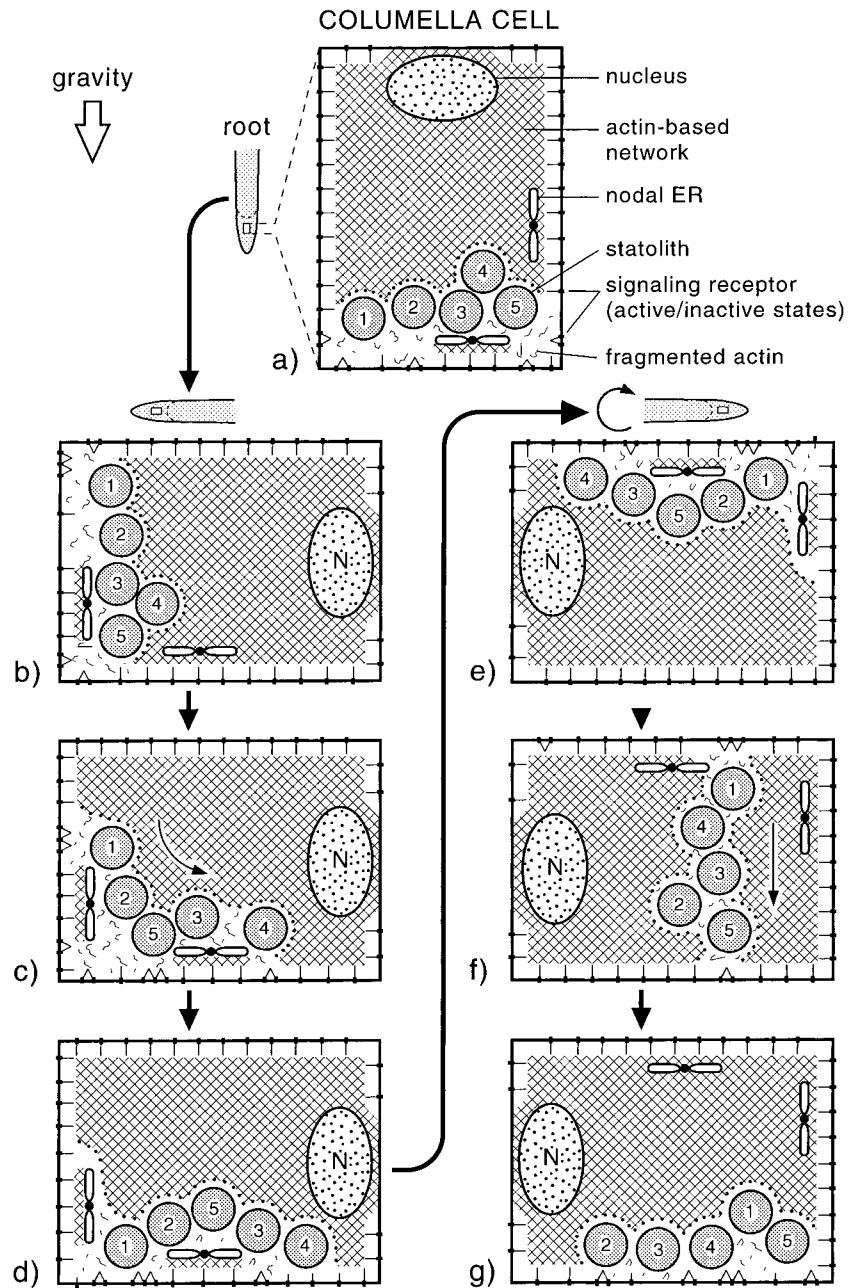
actin-based network that governs the access to this region. The sedimentation kinetics experiments, however, do not rule out the possible involvement of enzymes in aiding statolith sedimentation or statolith-mediated signaling to cell surface receptors. Several types of enzymes are known to participate in the regulation of the spatial and temporal organization of actin filaments in cells, and this regulated assembly and disassembly has been shown to be of crucial importance for many cellular functions.

A New Model of the Gravisensory Apparatus of Root Tip Columella Cells

As discussed in the preceding sections, the sedimentation behavior of the statoliths in maize columella cells and the physical simulation experiments reported here are inconsistent with gravisensing models in which the statoliths are tethered to the plasma membrane (or ER?) via actin filaments (Sievers et al., 1991; Baluska and Hasenstein, 1997). This has led us to formulate a new model of the gravisensory apparatus of columella cells, which is depicted in Figure 6. This model both illustrates the sedimentation trajectories of statoliths associated with root reorientation and suggests how the redistribution of statoliths may locally stimulate or inhibit stretch-activated receptors in the plasma membrane.

Central to this model is an actin-based cytoskeletal network that pervades the entire cytoplasm and is more extensive and coherent in the central, ER-devoid region of the cell (Fig. 4). The network is postulated to be linked to stretch-sensitive receptors in the plasma membrane and to interact with cortical microtubules and other cellular structures to form a tensegrity-like force interaction system in which tension is continuously transmitted across all structural members (Ingber, 1993; Ingber et al., 1994; Ingber, 1998). Unlike other, non-sedimentable organelles of columella cells such as the nucleus, the amyloplast-type statoliths are postulated to have no physical links to the components of the cytoskeletal network but instead to function by locally disrupting the network. Thus, when the statoliths become redistributed in response to a change in the gravity vector, they produce a signal both by altering the distribution of tension within the cytoskeletal network as a whole and by changing the overall distribution of links between the network and the stretch-sensitive receptors in the plasma membrane. The directionality of this signal would be mediated primarily by the changes in the distribution of the links between the network and the plasma membrane and refined by the distribution of "nodal ER" domains (Zheng and Staehelin, 2001). The nodal ER domains are structurally unique ER domains of columella cells that consist of groups of usually five to seven sheet-like, rough ER membranes that are connected to each other through a central nodal rod much like the

Figure 6. Tensegrity-based model of the gravi-sensing apparatus of columella cells. The model depicts an actin-based cytoskeletal network (cross-hatched lines) that pervades the entire cytoplasm, is denser in the cell center than in the cell periphery, and is coupled to stretch-sensitive receptors in the plasma membrane. The amyloplast-type statoliths are postulated to be not linked directly to the cytoskeletal network but to activate/inactivate the receptors by locally disrupting the network and thereby affecting the tensional forces within the network. The asymmetrically organized nodal ER domains shield local plasma membranes from approaching statoliths and may provide a directionality vector to the sensing system. A through G, Behavior of statoliths during the reorientation of a root. The cell periphery contains fewer obstructions to statolith movement than the cell center, and the statoliths preferentially travel within this region. In side-to-side sedimentation experiments (E, F, and G), the statoliths first move horizontally toward forming “channels” before they pass through the channels to the lower side of the cell.



attachment of petals to a flower base. These mechanically stable ER membrane domains can be distinguished from the more tubular cortical ER cisternae by being positioned at a specific distance from the plasma membrane, and by being spatially organized in a cell position-dependent manner within the columella tissue. Electron micrographs of cryofixed/freeze-substituted cells show that the nodal ER membranes can prevent the statoliths from approaching the plasma membrane in localized areas. Such asymmetrically distributed, unperturbed plasma membrane domains could allow the columella region as a whole to recognize the exact orientation of the root with respect to the gravity vector and to produce

differential signals for the upper and lower parts of the reoriented root (Zheng and Staehelin, 2001).

In all cells investigated to date, actin filaments form tight, regulated associations with the plasma membrane (Alberts et al., 1994). Although nothing is known about molecules that may mediate and regulate actin-plasma membrane interactions in columella cells, such molecules have been investigated in considerable detail in other systems (Tsukita et al., 1997). The ezrin/radixin/moesin proteins, which are also related to the actin/glycophorin C-binding band 4.1 protein of erythrocytes, constitute the most prominent family of proteins that cross-link actin filaments to plasma membrane proteins in yeast and many

multicellular organisms. These proteins have an actin binding domain at their carboxyl terminus and a plasma membrane protein binding site at their amino terminus. For this reason, ezrin/radixin/moesin proteins are obvious candidates for connecting the actin-based cytoskeletal network of columella cells to the plasma membrane. Because they can be converted from a free to an actin/plasma membrane binding state by either protein phosphorylation or phosphoinositide binding, it is not difficult to conceive how they may participate in a gravitropic signaling system.

Evaluation of the Tensegrity Model of Gravisensing in the Context of Gravisensing Kinetics and Microgravity Experiments

The value of any new model rests on its ability to account for critical experimental findings and its potential for generating novel experimental hypotheses. Here we discuss briefly how the tensegrity model can explain (a) the rapid changes in membrane potentials after gravistimulation, (b) the gravitropic responses of plants containing starch-deficient statoliths, (c) the behavior of statoliths under microgravity conditions, and (d) the effects of CD on gravitropism.

How well can this model account for the rapid changes in membrane potential of statocytes after tilting of a root, which in *Lepidium* can occur in as little as 8 s (Behrens et al., 1985). One of the hallmarks of a tensegrity system is its ability to rapidly transmit a local change in tension to the network as a whole and to concomitantly undergo shape changes. Thus, though the actin-tethered statolith model could in theory rapidly transmit a signal to the cell surface, the number of tethers required to ensure signaling in all directions would, according to our calculations, severely reduce the ability of the statoliths to sediment.

The new model is also compatible with the reported reduced, but not absent, gravitropic responses of plants that possess starch-deficient statoliths (Caspar and Pickard, 1989; Kiss et al., 1989; Kiss et al., 1996). As discussed by Sack (1997), the reduced sensing responses of such mutants can be attributed to the loss of starch and the resulting reduction in amyloplast mass and are not due to secondary mutations. Thus, although the amount of statolith sedimentation is greatly reduced in these mutants, the limited sedimentation that does occur (Kiss et al., 1989; Kiss et al., 1996) could perturb a tensegrity-based cytoskeletal system sufficiently to affect the tension in the network as a whole and thereby trigger a muted response (Ingber, 1993; Ingber et al., 1994).

Microgravity-based studies of statolith behavior in columella cells have yielded several observations that have been interpreted to support the actin-tether model of gravitropic sensing (Perbal et al., 1997), but

can equally well be accounted for by our tensegrity-based model. For example, during parabolic flights, initially sedimented statoliths were observed to move toward the cell center as soon as the seedlings were exposed to several minutes of microgravity (Volkmann et al., 1991). In a study of white clover seedlings grown and fixed under microgravity conditions, Smith et al. (1997) similarly observed that in serially sectioned and computer-reconstructed groups of columella cells the statoliths became clustered near the cell center. This finding led the authors to suggest that the statoliths may be held together by cross-linking microfilaments, which would increase the coherence of the response of the gravitropic signaling system and thereby its signal-to-noise ratio. However, the clustering behavior can be equally well explained by a model in which the non-tethered statoliths are excluded from the actin-based network to minimize the energetically unfavorable interface between the network and the grouped statoliths.

Several studies of the effects of CD on root gravitropism have been published, but the results are contradictory. Thus, whereas Blancaflor and Hasenstein (1997) and Staves et al. (1997) have reported that CD applied at concentrations of 10 and 20 μM , respectively, do not inhibit root gravitropism, Guikema and Gallegos (1992) have shown that when CD is applied in agar blocks at higher concentrations to root caps, the roots lose their ability to directionally reorient in response to a change in the gravitational field.

In the context of our studies, we do not feel that the relative insensitivity of the gravisensing apparatus of columella cells to CD contradicts our findings or our model. Indeed, we believe that our model is vindicated by the CD data mentioned above. A system based on discreet actin links between statoliths and/or plasma membrane would exhibit a loss of gravitropic signaling very quickly in the presence of CD. However, our model, which involves an actin-based tensegrity type of network, would provide a redundant and integrated mechanism for statolith gravity perception that would require higher concentrations of CD to become degraded.

MATERIALS AND METHODS

Videomicroscopy of Living Cells

Seeds of corn (*Zea mays* L. cv Yellow Dent; East Texas Seed Company, Tyler, TX) were germinated in darkness between sheets of filter paper moistened with ultra-filtered water in vertically positioned Petri dishes. The dishes were kept at $25^{\circ}\text{C} \pm 1.5^{\circ}\text{C}$. After 48 to 50 h of germination, primary roots in three different length categories were selected; 20- to 29-mm lengths, 30- to 39-mm lengths, and 40- to 55-mm lengths. The distal 5 mm of the root tips were sectioned using a Leica VT1000M vibratome. Section thickness ranged from 50 to 60 μm , with the goal of leaving one to two layers of intact columella cells within the section (Sack et al., 1986). The vibratome buffer solution

consisted of 0.5 mM KCl, 0.1 mM CaCl₂, 0.1 mM MgCl₂, 0.5 mM NaCl, and 1.0 mM MES [2-(*N*-morpholino)ethanesulfonic acid] buffer at pH 6.8.

Videomicroscopy of amyloplast motion was conducted with a light microscope (Standard-14, Zeiss, Jena, Germany) fitted with a video relay lens/C-mount (Edmund Scientific, Barrington, NJ) and a video camera (series 68, Dage-MTI, Inc., Michigan City, IN). The entire microscope, specimen stage, and video camera were mounted on a platform constructed to allow the rotation of sections, the microscope, and the camera as a unit, thereby orienting the columella cells within the sections at any angle with respect to gravity. Sections were placed on glass slides and mounted with respect to gravity in such a way as to ensure proper initial orientations for sedimentation. To fully explore the movement of plastids throughout the cell, amyloplast dynamics were recorded during sedimentation along three different profiles: from the distal end to a lateral side (section initially placed vertical and subsequently rotated 90°, the distal-to-side profile), from the distal end to the basal end (section initially placed vertical and subsequently inverted [rotated 180°, the distal-to-basal profile]), and from a lateral side to the opposing lateral side (section initially placed horizontal and subsequently rotated 180°, the side-to-side profile).

Quantitative Image Analysis

MetaMorph (version 3.0, Universal Imaging Corporation, Downingtown, PA) imaging software was used to control and capture the video images. In preliminary studies we determined that the statoliths showed negligible position changes in less than 20 s; therefore, still images at 15- to 30-s intervals were acquired for digital processing. Horizontal and vertical coordinates of individual amyloplast centers over the entire time span of sedimentation were determined using NIH Image software (version 1.67, developed at the United States National Institutes of Health and available on the Internet at <http://rsb.info.nih.gov/nih-image>). Only viable cells from the second or third story of mature columella cells were selected for data analysis. To analyze the dynamics of sedimentation, these coordinate-time data were processed and visualized graphically using custom MATLAB software.

Figure 7A shows the coordinate system used by the custom analysis software. Absolute (non-directional) velocity and the velocities along the *x* (horizontal) and *y* (vertical) axes were analyzed throughout the entire sedimentation time. Velocity was computed as the average velocity achieved between captured video frames. The velocity characteristics observed in samples from the three root-length categories were compared. The velocity characteristics during the first third of the total sedimentation time were compared with characteristics observed in the middle and final third time periods. The same length categories and sedimentation profiles were investigated for sections treated with CD (section bathed in a solution of 100 μM CD, 1% [w/v] dimethyl sulfoxide, for 1 h prior to video). The analysis software compiled velocity data, and

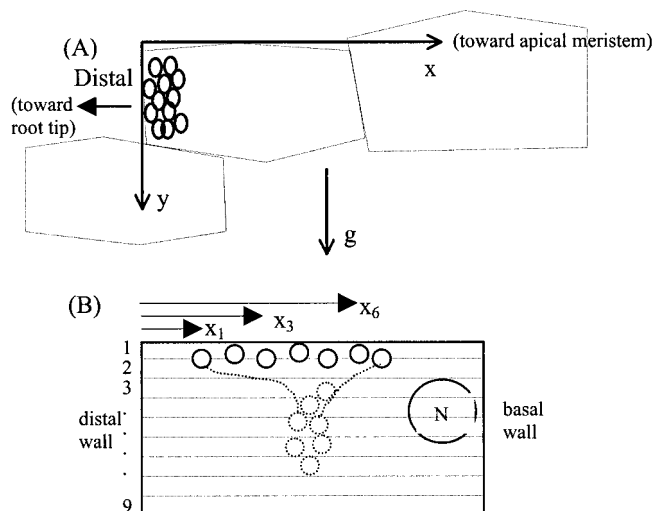


Figure 7. Geometry used for characterizing statolith velocity and channeling behavior. A, Coordinate system used for amyloplast sedimentation analysis. The *y* axis is parallel to the gravity vector. The *x* axis, chosen to parallel the side of the columella cell opposite and perpendicular to the gravity vector, creates a right-handed coordinate system with the *z* axis (not shown) into the columella cells. By drawing the coordinate system tangent with the outermost cell wall of the columella cell, the coordinate axes approximate the upper and distal boundaries of the simplified rectangular cell. B, Geometry used to compute the CC in Equation 3 with the cell divided into nine segments and each statolith identified by a subscript.

the data were formulated into practical quantifications of three statolith behavior questions as follows.

Quantitative Analysis of Statolith Behaviors

Behavior 1

Do statoliths fall, unobstructed, directly along the gravity vector or via obstructed paths through channels? Deviation from unobstructed sedimentation was quantified using a CC (Eq. 3), which is a measure of the variance of the *x* position (normal to gravity) of *n* statoliths passing downward through nine sectors (each 2 μm in width) of the cell as illustrated in Figure 7B. CC_{top} is the variance in *x* position in the top division, x_i is the position of a statolith *i* within a specific division, \bar{x} is the mean *x* position of all statoliths within that same division, and *n* is the total instantaneous number of statoliths passing through that division. Thus, perfectly vertical sedimentation would give $CC = 1.0$, whereas obstructions forcing statoliths together would give $CC < 1.0$, and obstructions forcing them apart would give $CC > 1.0$. Therefore, CC is a measure of the degree of lateral displacement during sedimentation of all statoliths tracked within a cell:

$$CC = \frac{\sum_{i=1}^n (x_i - \bar{x})^2}{n - 1} / CC_{top} \quad (3)$$

Behavior 2

Do statoliths sediment independently or does the trajectory of one depend on the trajectories of others? Correlation coefficients, the covariance between individual amyloplasts divided by their standard deviations (Eq. 4), were computed for both position over time ($\Delta x/\Delta t$, velocity correlation) and velocity over time ($\Delta v/\Delta t$, correlation). A correlation coefficient of 1.0 indicates perfect linear correlation of velocity ($\Delta v/\Delta t$) between two statoliths. Correlation matrices were constructed so that each statolith could be correlated with all other statoliths in a given columella cell.

Correlation Coefficient(i, j) =

$$\frac{\text{Covariance}(i, j)}{\sqrt{\text{Covariance}(i, i) \cdot \text{Covariance}(j, j)}} \quad (4)$$

Behavior 3

Do statoliths sediment at constant velocity or at a sedimentation velocity that changes systematically over the downward trajectory? The vertical range of statolith sedimentation was divided into five equally wide regions from the upper to the lower sides of the cell, as in Figure 7B, but with five rather than nine regions. The average and SD of y velocity of all statoliths was determined in each region and presented in the form of vertical histograms.

Electron Microscopy

Following 48 h of germination, seedlings selected for electron microscopy were transferred to a sterile 0.1 M Suc solution at ambient temperature without light for 12 h. This treatment increases the yield of well-frozen samples by increasing the solute concentration in the cells and thereby reducing the amount of ice crystal damage during freeze fixation. Specimens were prepared from 1-mm-thick slices of 35- to 45-mm-long roots while submerged in the Suc solution and mounted in high-pressure freezing specimen cups coated with lecithin (Craig and Staehelin, 1988). Frozen samples were substituted in 4% (w/v) OsO₄ in acetone at -80°C for 3 d, -20°C for 1 d, 4°C overnight, washed with cold acetone at 4°C, and stained en bloc with saturated uranyl acetate in acetone for 6 h at 4°C. After a dry acetone wash at room temperature, the samples were infiltrated in Spurr's resin and polymerized at 70°C for 8 h. The 70-nm-thick sections were stained with uranyl acetate in 70% (v/v) methanol for 10 min, lead citrate for 4 min, and examined at 80 kV in an electron microscope (model CM 10, Philips, Eindhoven, The Netherlands).

ACKNOWLEDGMENT

We thank Dr. Mark Dubin for insightful comments on the manuscript.

Received October 31, 2000; accepted November 2, 2000.

LITERATURE CITED

- Alberts B, Bray D, Lewis J, Raff M, Roberts K, Watson JD** (1994) *Molecular Biology of the Cell*. Garland Publishing, New York
- Baluska F, Hasenstein KH** (1997) Root cytoskeleton: its role in perception of and response to gravity. *Planta* **203**: S69-S78
- Baluska F, Hauskrecht M, Barlow PW, Sievers A** (1996) Gravitropism of the primary root of maize: a complex pattern of differential cellular growth in the cortex independent of the microtubular cytoskeleton. *Planta* **198**: 310-318
- Behrens HM, Gradmann D, Sievers A** (1985) Membrane-potential responses following gravistimulation in roots of *Lepidium sativum* L. *Planta* **163**: 463-472
- Björkman T** (1988) Perception of gravity by plants. *Adv Bot Res* **15**: 1-41
- Blancaflor EB, Fasano JM, Gilroy S** (1998) Mapping the functional roles of cap cells in the response of *Arabidopsis* primary roots to gravity. *Plant Physiol* **116**: 213-222
- Blancaflor EB, Hasenstein KH** (1997) The organization of the actin cytoskeleton in vertical and graviresponding primary roots of maize. *Plant Physiol* **113**: 1447-1455
- Caspar T, Pickard BG** (1989) Gravitropism in a starchless mutant of *Arabidopsis*. *Planta* **177**: 185-197
- Chen R, Rosen E, Masson PH** (1999) Gravitropism in higher plants. *Plant Physiol* **120**: 343-350
- Craig S, Staehelin LA** (1988) High pressure freezing of intact plant tissue. *Eur J Cell Biol* **46**: 80-93
- Darwin F** (1903) The statolith theory of geotropism. *Nature* **67**: 571-572
- Driss-Ecole D, Vassy J, Rembur J, Guivarc'h A, Prouteau M, Dewitte W, Perbal G** (2000) Immunolocalization of actin in root statocytes of *Lens culinaris* L. *J Exp Bot* **51**: 521-528
- Gittes F, Mickey B, Nettleton J, Howard J** (1993) Flexural rigidity of microtubules and actin filaments measured from thermal fluctuations in shape. *J Cell Biol* **120**: 923-934
- Guikema JA, Gallegos GL** (1992) Plastids: dynamic components of plant cell development. *Trans Kans Acad Sci* **95**: 50-54
- Haberlandt G** (1900) Über die perzeption des geotropischen reizes. *Ber Dtsch Bot Ges* **18**: 261-272
- Ingber DE** (1993) Cellular tensegrity: defining new rules of biological design that govern the cytoskeleton. *J Cell Sci* **104**: 613-627
- Ingber DE** (1998) The architecture of life. *Sci Am* **278**: 30-39
- Ingber DE, Dike L, Hansen L, Karp S, Liley H, Maniotis A, McNamee H** (1994) Cellular tensegrity: exploring how mechanical changes in the cytoskeleton regulate cell growth, migration, and tissue pattern during morphogenesis. *Int Rev Cytol* **150**: 173-224
- Janmey PA, Euteneuer U, Traub P, Schliwa M** (1991) Viscoelastic properties of vimentin compared with other filamentous biopolymer networks. *J Cell Biol* **113**: 155-160
- Kiss JZ, Hertel R, Sack FD** (1989) Amyloplasts are necessary for full gravitropic sensitivity in roots of *Arabidopsis thaliana*. *Planta* **177**: 198-206

- Kiss JZ, Wright JB, Caspar T** (1996) Gravitropism in roots of intermediate-starch mutants of *Arabidopsis*. *Physiol Plant* **97**: 237–244
- Konings H** (1995) Gravitropism of roots: an evaluation of progress during the last three decades. *Acta Bot Neerl* **44**: 195–223
- Kuznetsov OA, Hasenstein KH** (1996) Intracellular magnetophoresis of amyloplasts and induction of root curvature. *Planta* **198**: 87–94
- Leach HW, Schoch TJ** (1961) Structure of the starch granule: II. Action of various amylases on granular starches. *Cereal Chem* **38**: 34–46
- Moore R** (1986) A morphometric analysis of the redistribution of organelles in columella cells of horizontally-oriented roots of *Zea mays*. *Ann Bot* **57**: 119–131
- Moore R, Evans ML** (1986) How plants perceive and respond to gravity. *Am J Bot* **73**: 574–587
- Nemec B** (1900) Über die art der wahrnehmung des schwerkräftes bei den pflanzen. *Ber Dtsch Bot Ges* **18**: 241–245
- Perbal G, Driss-Ecole D, Tewinkel M, Volkmann D** (1997) Statocyte polarity and gravisensitivity in seedling roots grown in microgravity. *Planta* **203**: S57–S62
- Pilet PE** (1971) Root cap and georeaction. *Nat New Biol* **233**: 83
- Robinson DG** (1985) *Plant Membranes*. John Wiley & Sons, New York
- Sack FD** (1994) Cell biology of plant gravity sensing. *Adv Space Res* **14**: 117–119
- Sack FD** (1997) Plastids and gravitropic sensing. *Planta* **203**: S63–S68
- Sack FD, Suyemoto MM, Leopold AC** (1985) Amyloplast sedimentation kinetics in gravistimulated maize roots. *Planta* **165**: 295–300
- Sack FD, Suyemoto MM, Leopold AC** (1986) Amyloplast sedimentation and organelle saltation in living corn columella cells. *Am J Bot* **73**: 1692–1698
- Sievers A, Buchen B, Volkmann D, Hejnowicz Z** (1991) Role of the cytoskeleton in gravity perception. *In* CW Lloyd, ed, *The Cytoskeletal Basis of Plant Growth and Form*. Academic Press, London
- Sievers A, Kruse S, Kuo-Huang L, Wendt M** (1989) Statoliths and microfilaments in plant cells. *Planta* **179**: 275–278
- Smith JD** (1996) Plant gravity perception and sensitivity control under low-gravity and clinorotated conditions. PhD thesis. University of Colorado, Boulder
- Smith JD, Todd P, Staehelin LA** (1997) Modulation of statolith mass and grouping in white clover (*Trifolium repens*) grown in 1-g, microgravity and on a clinostat. *Plant J* **12**: 1361–1373
- Staves MP, Wayne R, Leopold AC** (1997) Cytochalasin D does not inhibit gravitropism in roots. *Am J Bot* **84**: 1530–1535
- Stockus A** (1994) Basic assumptions and comparison of three gravitropic response models. *Adv Space Res* **14**: 145–148
- Theriot JA, Mitchinson TJ** (1991) Actin microfilament dynamics in locomoting cells. *Nature* **352**: 126–131
- Todd P** (1994) Mechanical analysis of statolith action in roots and rhizoids. *Adv Space Res* **14**: 121–124
- Tsukita S, Yonemura S, Tsukita S** (1997) ERM proteins: head-to-tail regulation of actin-plasma membrane interaction. *Trends Biochem Sci* **22**: 53–58
- Volkmann D, Buchen B, Hejnowicz Z, Tewinkel M, Sievers A** (1991) Oriented movement of statoliths studied in a reduced gravitational field during parabolic flights of rockets. *Planta* **185**: 153–161
- Wacksstock DH, Schwartz WH, Pollard TD** (1994) Cross-linker dynamics determine the mechanical properties of actin gels. *Biophys J* **66**: 801–809
- Wayne R, Staves MP, Leopold AC** (1990) Gravity-dependent polarity of cytoplasmic streaming in *Nitellopsis*. *Protoplasma* **155**: 43–57
- Zheng H-Q, Staehelin LA** (2001) Nodal ER, a novel form of ER found exclusively in gravity-sensing columella cells. *Plant Physiol* **125**: 252–265